Chemistry & Biology
Article

Covalent Inhibitors of Human Monoacylglycerol Lipase: Ligand-Assisted Characterization of the Catalytic Site by Mass Spectrometry and Mutational Analysis

Nikolai Zvonok,[1] Lakshmipathi Pandarinathan,[1] John Williams,[1,2] Meghan Johnston,[1,2] Ioannis Karageorgos,[1] David R. Janero,[1,*] Srinivasan C. Krishnan,[3] and Alexandros Makriyannis[1,*]
[1]Center for Drug Discovery, Northeastern University, 116 Mugar Hall, 360 Huntington Avenue, Boston, MA 02115, USA
[2]Department of Chemistry and Chemical Biology, Northeastern University, Boston, MA 02115, USA
[3]Applied Biosystems, 500 Old Connecticut Path, Framingham, MA 01701, USA
*Correspondence: d.janero@neu.edu (D.R.J.), a.makriyannis@neu.edu (A.M.)
DOI 10.1016/j.chembiol.2008.06.008

SUMMARY

The active site of recombinant hexa-histidine-tagged human monoacylglycerol lipase (hMGL) is characterized by mass spectrometry using the inhibitors 5-((biphenyl-4-yl)methyl)-*N,N*-dimethyl-2*H*-tetrazole-2-carboxamide (AM6701), and *N*-arachidonylmaleimide (NAM) as probes. Carbamylation of Ser^{129} by AM6701 in the putative hMGL catalytic triad demonstrates this residue's essential role in catalysis. Partial NAM alkylation of hMGL cysteine residues 215 and/or 249 was sufficient to achieve ~80% enzyme inhibition. Although Cys^{215} and/or Cys^{249} mutations to alanine(s) did not affect hMGL hydrolytic activity as compared with nonmutated hMGL, the C215A displayed heightened NAM sensitivity, whereas the C249A evidenced reduced NAM sensitivity. These data conclusively demonstrate a sulfhydryl-based mechanism for NAM inhibition of hMGL in which Cys^{249} is of paramount importance. Identification of amino acids critical to the catalytic activity and pharmacological modulation of hMGL informs the design of selective MGL inhibitors as potential drugs.

INTRODUCTION

Cannabinoid receptors, their endogenous ligands (endocannabinoids), and the enzymes responsible for endocannabinoid synthesis and deactivation comprise a ubiquitous mammalian signaling system that regulates diverse physiological functions. The principal endocannabinoids, *N*-arachidonoylethanolamine (anandamide, AEA) (Devane et al., 1992) and 2-arachidonoylglycerol (2-AG) (Mechoulam et al., 1995; Sugiura et al., 1995), are produced on demand as cannabinoid-receptor activating ligands having distinctive pharmacological profiles. Because unregulated endocannabinoid signaling can have adverse consequences, endocannabinoid concentrations are tightly and redundantly controlled at points of synthesis, transport, and biotransformation of the associated signaling lipids (Di Marzo and Petrosino, 2007). Enzymatic endocanabinoid deactivation is key to attenuating endocannabinoid signaling. Fatty acid amide hydrolase (FAAH) is an integral membrane amidase primarily responsible for AEA hydrolysis that may exist in multiple isoforms (Cravatt et al., 1996; Wei et al., 2006). Although FAAH also metabolizes 2-AG in vitro (Goparaju et al., 1998), soluble monoacylglycerol lipase (MGL) serves as the major enzyme for 2-AG deactivation in cells (Dinh et al., 2004), perhaps along with subsidiary MGL-like esterases (Muccioli et al., 2007; Blankman et al., 2007).

Agents that modulate endocannabinoid system transmission are actively being sought as therapeutics to treat important behavioral, metabolic, and neurological diseases (Vemuri et al., 2008; Pacher et al., 2006). For therapeutic upregulation of endocananbinoid signaling, pharmacological inhibition of endocannabinoid deactivating enzymes may offer more selectivity and less risk of unwanted psychotropic side effects as compared with cannabinoid-receptor agonists (Malan et al., 2003). Specifically, targeted inhibition of 2-AG deactivation is considered an attractive therapeutic approach against pain, inflammation, and neurodegenerative and immune disorders (Pacher et al., 2006; Saario and Laitinen, 2007). Although many available FAAH inhibitors also act on MGL (Deutsch et al., 1997; Ghafouri et al., 2004), high-affinity ligands that potently and selectively inhibit MGL are currently lacking. The molecular mechanisms of known MGL inhibitors are speculative, having been inferred mainly by analogy from MGL modeling studies with or without virtual screening (Karlsson et al., 1997; Saario et al., 2006). A putative MGL catalytic triad (Ser^{122} … Asp^{239} … His^{269}) has been predicted from homology with other serine hydrolases and limited site-directed mutagenesis experiments (Karlsson et al., 1997). However, direct experimental demonstration of the involvement of these (or other) amino acid residues in pharmacological MGL inhibition is lacking.

First described as a putative competitive inhibitor of AEA transport (IC_{50} = 270 pM in a cellular assay) with analgesic activity in rodents (Moore et al., 2005), LY2183240 was subsequently shown to target mouse-brain FAAH ($IC_{50} \approx 13$ nM) and recombinant MGL ($IC_{50} \approx 5.3$ nM) in a time-dependent manner (Alexander and Cravatt, 2006). FAAH inhibition by LY2183240 was postulated to involve carbamylation of active-site Ser^{241} (Alexander and Cravatt, 2006). However, the molecular details of MGL inhibition by LY2183240 remain unknown. In addition, Ortar et al. (2008) have recently demonstrated that LY2183240 consists of two isomers, as we have confirmed in the course of LY2183240 synthesis and purification for the present work (data not shown).

Substituted maleimide derivatives including NAM inhibit incompletely MGL-like enzymatic activity in rat cerebellar membranes (Saario et al., 2005) and rat adipocyte subcellular fractions (Sakurada and Noma, 1981). As with inhibition of MGL by LY2183240, no experimental evidence is available regarding the mechanism of MGL inhibition by NAM. The conjugated double bond of *N*-substituted maleimides can undergo a facile Michael addition to nucleophilic groups of amino acids and, particularly, the thiol group of cysteine (Smyth et al., 1960). Consequently, NAM's inhibition of MGL in rat cerebellar membranes was hypothesized from molecular modeling studies to reflect an interaction between NAM and either Cys^{242} or Cys^{208}, these two of the enzyme's six cysteine residues having been modeled proximally to the putative substrate-binding site (Saario et al., 2005). There are four cysteine residues in human MGL, and their thiol groups are not involved in disulfide bond formation (Zvonok et al., 2008).

In the present study, we show that the 2,5-LY2183240 isomer 5-((biphenyl-4-yl)methyl)-*N,N*-dimethyl-2*H*-tetrazole-2-carboxamide (AM6701) is a more potent inhibitor of recombinant hexahistidine-tagged human MGL (hMGL) than the 1,5-isomer 5-((biphenyl-4-yl)methyl)-*N,N*-dimethyl-1*H*-tetrazole-1-carboxamide (AM6702). We have therefore characterized AM6701-inhibited hMGL through a comprehensive mass spectrometric (MS) analysis to identify directly the amino acid residue(s) involved. We have also successfully applied this ligand-assisted protein structure (LAPS) approach to obtain the first direct structural information on hMGL inhibition by NAM, which we have augmented with site-directed mutagenesis data. The results are of value in identifying specific amino acid residues critical to MGL catalysis and pharmacological modulation, informing thereby the rational design of selective MGL inhibitors with potential therapeutic utility.

RESULTS AND DISCUSSION

hMGL Inhibition by AM6701 and NAM

SDS-PAGE followed by either Coomassie staining or western blot anti-5-His antibody detection demonstrated that the hMGL overexpressed in *E. coli* and isolated by immobilized metal-affinity chromatography is a single monomeric protein with an estimated molecular mass, ≈35 kDa, that approximates the calculated mass of 34,123 kDa (Figures 1A and 1B). The catalytic properties of purified hMGL are similar to those of the homologous, soluble crude rMGL using either 2-AG or a novel fluorogenic reporter, arachidonoyl,7-hydroxy-6-methoxy-4-methylcoumarin ester (AHMMCE), as substrate (Zvonok et al., 2008). With a sensitive fluorescence-based assay, the inhibitor profiles of both LY2183240 isomers and NAM were first characterized using *E. coli* lysate (containing hMGL) and soluble crude rMGL as enzyme sources. After 3 hr incubation, the LY2183240 isomers AM6701 and AM6702 inhibited hMGL in the nanomolar range with concentration dependence, whereas NAM was markedly less potent (Figure 1C). Only the LY2183240 2,5-regioisomer (AM6701) inhibited both hMGL and soluble crude rMGL with low nM IC_{50}s, making AM6701 the more potent LY2183240 isomer as well as the most potent MGL inhibitor profiled (Figure 1D). The high potency of AM6701 as MGL inhibitor relative to both AM6702 and NAM is supported by published studies using 2-AG as substrate, albeit with varying sources of crude MGL(-like) activity (Ortar et al., 2008; Saario et al., 2005; Figure 1D).

We next defined conditions that would elicit maximal hMGL inhibition by either AM6701 or NAM so as to generate, efficiently, enzyme preparations useful for identifying the amino acid residue(s) critical to each inhibitor's action by MALDI-TOF MS. At a fixed substrate concentration of 50 μM AHMMCE, inhibition of purified hMGL was dependent upon the inhibitor:hMGL molar ratio (Table 1). Even at an equimolar ratio with hMGL, AM6701 markedly inhibited (by ~72%) the enzyme. Maximal inhibition (~90%) of hMGL by AM6701 was attained at an 8.3-fold molar excess of AM6701 over hMGL. In contrast, an equimolar ratio of NAM to hMGL resulted in only ~50% inhibition. A 3.3:1 NAM:hMGL molar ratio potentiated enzyme inhibition to ~80%, whereas up to a 33-fold molar excess of NAM elicited little further hMGL inhibition. Identical results were obtained at a fixed substrate concentration of 100 μM AHMMCE (data not shown). Consequently, we elected to incubate hMGL for 1 hr with an 8.3-fold molar excess of AM6701 to characterize by MALDI-TOF MS all inhibitor-related enzyme modification(s). Because of the relatively more pronounced concentration-dependence by which NAM inhibited hMGL hydrolysis of fluorogenic reporter AHMMCE (Table 1), the mechanism of hMGL inhibition by NAM was studied at the various NAM:hMGL molar ratios specified in Tables 1 and 2.

MS Analysis of hMGL Inhibition by AM6701

Desalted samples of untreated hMGL and enzyme that had been inhibited >90% by a 1 hr preincubation with an 8.3-fold molar excess of AM6701 were subjected overnight to in-solution trypsin digestion prior to MALDI-TOF MS analysis. A comparison of the spectra of the tryptic digest from naive and AM6701-inhibited hMGL revealed in the latter only one peptide with a 71 Da mass increase, which was provisionally attributed to the addition of a single dimethylcarbamyl group to the enzyme (Figure 2A). The carbamylation product was sensitive to the dithiothreitol-iodoacetamide treatment typically employed to disrupt disulfide bonds and alkylate free sulfhydryls prior to trypsin digestion. To avoid complete removal of the carbamyl group from AM6701-inhibited hMGL, a limited 30 min dithiothreitol-iodoacetamide treatment (Figure 2A) was conducted prior to MALDI-TOF MS. Under these mild conditions, ~30% of the peptide carbamylation observed in AM6701-inhibited hMGL was retained (Figure 2B).

Figure 3 depicts the MS/MS spectra of the 5247.87 *m/z* and 5318.79 *m/z* peptide ions derived from trypsin digests of naive (Figure 3A) and AM6701-inhibited (Figure 3B) hMGL, respectively. Although the precursor ions are intensive (Figure 2A and 2B), MS/MS spectral optimization is complicated by the high molecular weights involved, as reflected in the signal-to-noise ratio of the MS/MS spectra in Figures 3A and 3B. Nonetheless, the same fragmentation ions corresponding to the y ion for the sequence IAGGMSHG (Figure 3A) and the sequence IAGGM (Figure 3B) are identified. Notably, the masses for the last three residues (SHG) in the digest of AM6701-inhibited hMGL (Figure 3B) are 71 *m/z* greater than in the naive enzyme (Figure 3A). The high-resolution spectrum of the unmodified precursor ion at *m/z* 5247.87 (Figure 3A) corresponds to the tryptic peptide DYPGLPVFLLGH**S**MGGAIAILTAAERPGHFAGMVLI**S**PLVLANP E**S**ATTFKVLAAK (position 117-172), and the second ion at *m/z*

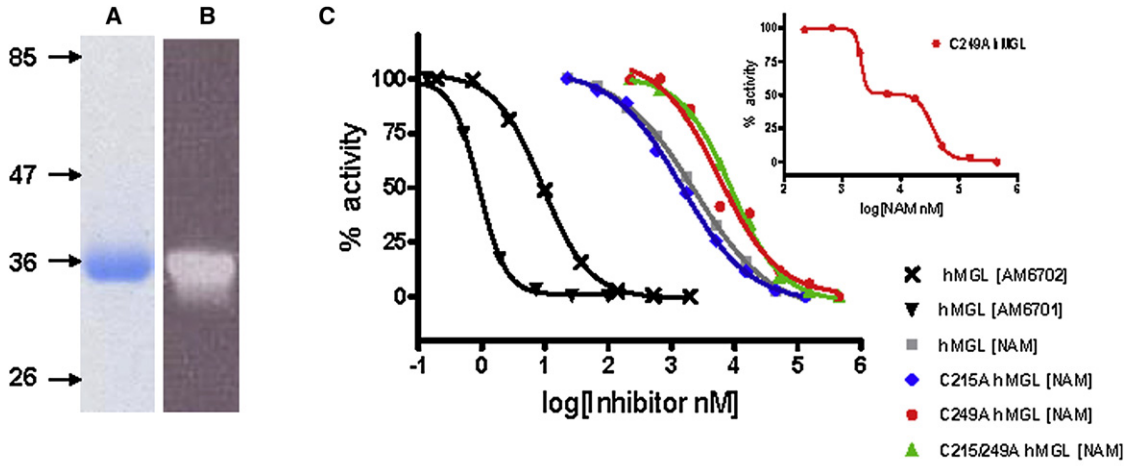

D

Inhibitor	IC_{50} rMGL[(1)]	IC_{50} hMGL[(1)]	IC_{50} MGL
AM6701	1.7 nM	0.9 nM	20.0 nM[(2)]
AM6702	100.0 nM	9.1 nM	8.1 μM[(2)]
NAM	n.d.	2.8 μM	0.140 μM[(3)]

[(1)] fluorescence-based assay of rMGL or hMGL with AHMMCE substrate

[(2)] radioactivity-based assay of cytosolic MGL from COS cells with [^{14}C]2-AG as substrate (Oktar et al., 2007)

[(3)] HPLC-based assay of MGL-like activity from rat cerebellum membranes with 2-AG as substrate (Saario et al., 2005)

n.d., not determined

Figure 1. Purification and Inhibition of hMGL

(A and B) (A) Coomassie stained 10% PAGE-SDS gel and (B) western blot analysis of IMAC-purified, recombinant hexa-histidine-tagged human MGL (hMGL).
(C) Best-fit, one-site plots of the concentration-dependent inhibition by AM6701, AM6702, and NAM of hMGL and designated hMGL cysteine mutants to hydrolyze AHMMCE. The inset highlights the biphasic nature of the hMGL C249A mutant by NAM as a two-site plot.
(D) IC_{50} values for inhibition of soluble crude rMGL, hMGL, and MGL prepared from COS cells and rat cerebellum by AM6701, AM6702, and NAM.

5318.79 is the carbamylated (+71 Da) product (Figure 3B). Because there are three serine residues in the tryptic fragment, tandem MS was performed on both the unmodified and modified ions to determine the exact serine residue modified by AM6701. Tandem MS unambiguously identified Ser^{129} as the hMGL residue carbamylated by AM6701. Mechanistically, the carbamylation product may arise from an attack by the Ser^{129} hydroxyl group on the AM6701 carbonyl moiety, the resultant carbamylated serine accounting for a 71 Da increase in the mass of the peptide (Figure 3C). Figure 3D (left panel) depicts schematically the spatial disposition of the amino acid residues Ser^{129} … Asp^{246} … His^{276} in the hMGL catalytic triad (Ser^{122} … Asp^{239} … His^{269} in human MGL) in an energetically favorable orientation with AM6701 before its reaction with enzyme. The carbamylated Ser^{129} residue in AM6701-inhibited hMGL is depicted in Figure 3D (right panel). These data clearly demonstrate the essential role of Ser^{129} in the conserved $G^{127}XSXG^{131}$ motif (i.e., $G^{120}XSXG^{124}$ in human MGL) of the catalytic triad for hMGL esterase activity.

MS and Mutational Analyses of hMGL Inhibition by NAM

The graded concentration dependence by which NAM inhibited hMGL activity (Figure 1 and Table 1) suggests the presence of high-affinity inhibitor binding site(s) that are in close proximity

Table 1. Concentration Dependence of hMGL Inhibition by AM6701 and NAM

Inhibitor	Inhibitor:hMGL Molar Ratio	hMGL Inhibition (%) 10 min
AM6701	1:1	72
	3.3:1	85
	8.3:1	91
NAM	1:1	51
	3.3:1	80
	8.3:1	82
	33:1	84

Reporter substrate (AHMMCE) concentration was 50 μM.

Table 2. Relative Content of NAM-Modified, Cysteine-Containing Peptides Identified by MS in Tryptic Digest of NAM-Treated hMGL

hMGL Cysteine Residues	*m/z*	Relative Percent Alkylation NAM:hMGL Ratio 8.3:1	33:1
Cys^{39}	3144.62; 3300.72	0	100[a]
Cys^{208}	2007.05	0	0[a]
Cys^{215}	2158.28	26[b]	22[b]
Cys^{249}	2445.38; 3534.97	74[b]	78[b]

[a] Percent alkylation of Cys^{39} relative to Cys^{208}.
[b] Percent alkylation of Cys^{215} relative to Cys^{249}.

to cysteine residues capable of interacting covalently with NAM and that may affect catalysis differentially. This suggestion is directly supported by MALDI-TOF MS analysis of cysteine-containing peptides in tryptic digests of NAM-inhibited hMGL (Figure 4A and 4B). At a NAM:hMGL molar ratio of 8.3:1, both unmodified and NAM-modified peptides at Cys^{215} or Cys^{249} were identified (Table 2), the latter evidencing a 369.27 Da mass increase. Even at the maximal, 33-fold NAM molar excess employed, comparable incomplete (84%) hMGL inhibition was observed, and Cys^{215} or Cys^{249} was still partially alkylated (Figure 4B). Based on the intensity of peptide signals in the MS spectra, the relative cysteine alkylation at positions 215 and 249 was similar at NAM:hMGL molar ratios of 8.3:1 (Cys^{215}, 26% and Cys^{249}, 74%) and 33:1 (Cys^{215}, 22% and Cys^{249}, 78%) (Table 2). Thus, a ~4-fold increase in NAM concentration affected neither the relative alkylation of Cys^{215} and Cys^{249} nor the degree

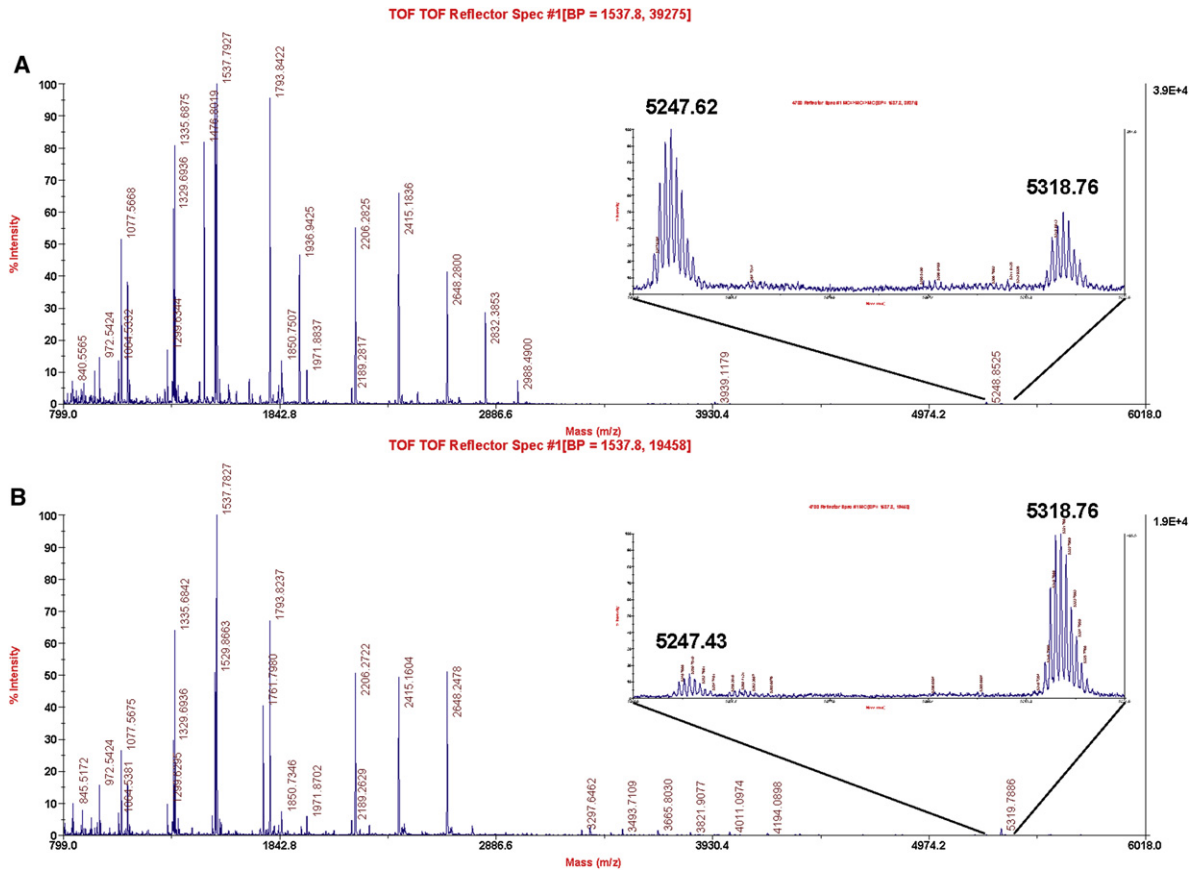

Figure 2. Peptide Fingerprinting of AM6701-Inhibited hMGL

The tryptic digest of the AM6701-inhibited hMGL was peptide fingerprinted using MALDI-TOF MS.
(A) The enzyme was subjected to mild reduction-alkylation before trypsin digestion.
(B) The enzyme was digested with trypsin without reduction-alkylation.
High-resolution MS spectra of the precursor ions are shown for the unmodified (*m/z* 5247.62) and carbamylated (*m/z* 5318.76) peptide DYPGLPVFLLGH**S**MGGAIAILTAAERPGHFAGMVLI**S**PLVLANPE**S**ATTFKVLAAK (position 117–172).

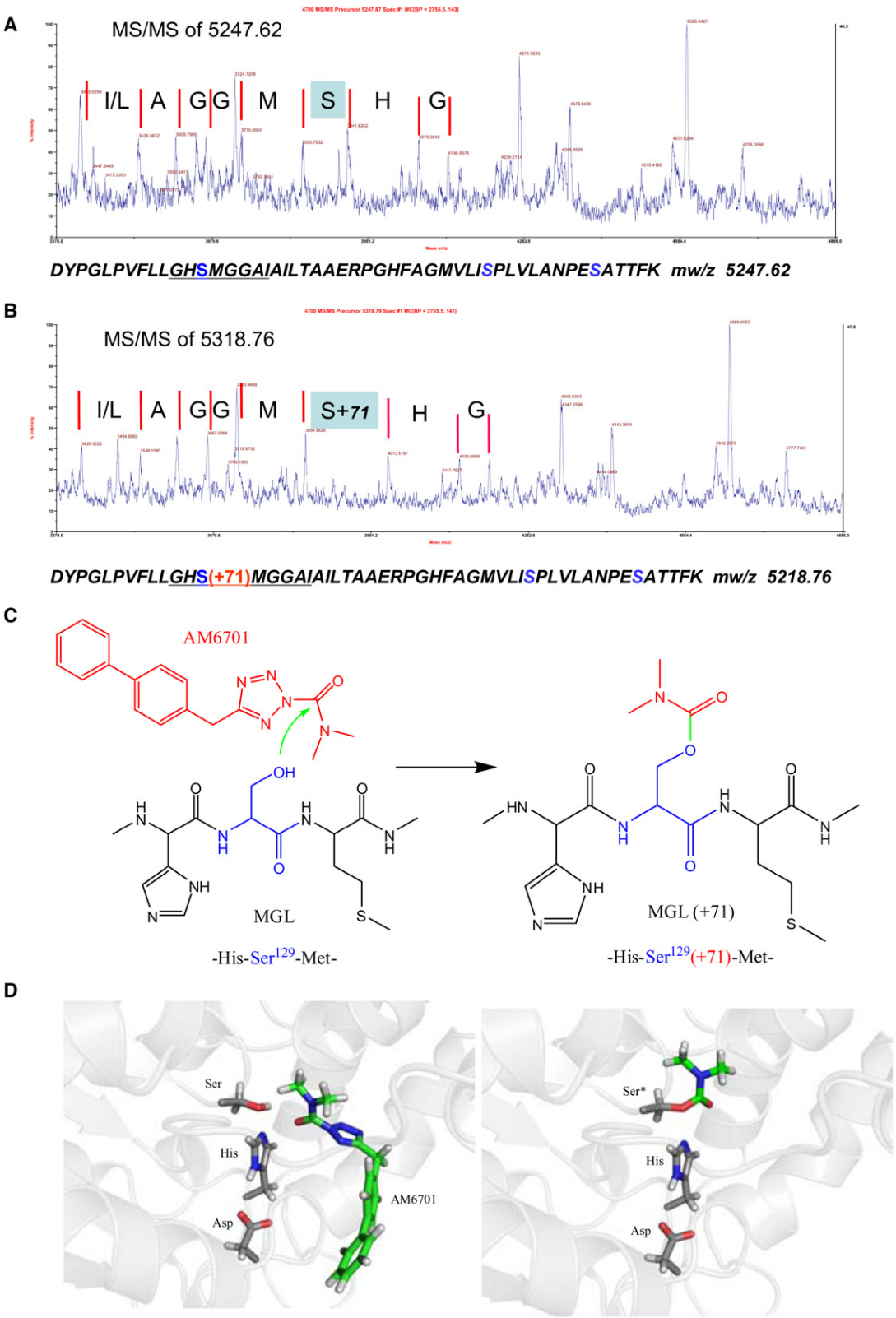

Figure 3. MALDI-TOF MS/MS Analysis of hMGL Carbamylation by AM6701

(A and B) Tandem MALDI-TOF MS/MS analysis of (A) unmodified and (B) modified peptides identified Ser^{129} as the hMGL residue carbamylated by AM6701. The fragmentation ions corresponding to the y-ion sequence IAGGMSHG and IAGGMS(+71)HG are underscored.

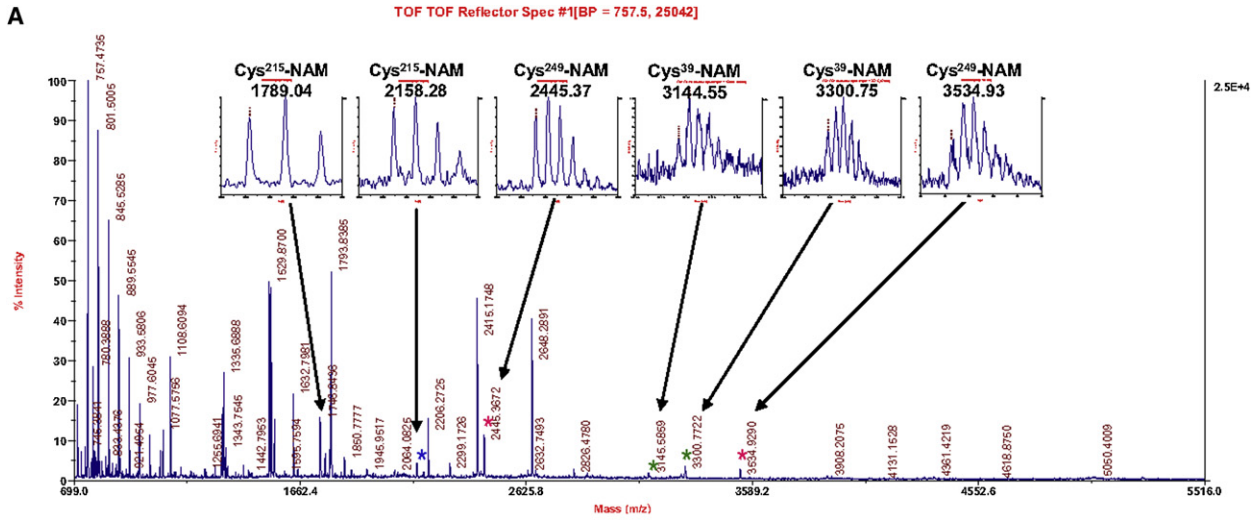

B

Detected (Da)	Theoretical (Da)	D (ppm)	Peptide Sequence	Position	Modification
3300.772	3300.724	-14.60	(R)/ RTPQSIPYQDLPHLVNADGQYLFC*R /(Y)	16-40	NAM
3144.551	3144.622	22.70	(R)/ TPQSIPYQDLPHLVNADGQYLFC*R /(Y)	17-40	NAM
1879.933	1879.922	-5.90	(R)/ NKTEVDIYNSDPLICR /(A)	194-209	
1637.800	1637.784	-9.80	(K)/ TEVDIYNSDPLICR /(A)	196-209	
1789.030	1789.015	-8.20	(R)/ AGLKVCFGIQLLNAVSR /(V)	210-226	
2158.276	2158.282	2.70	(R)/ AGLKVC*FGIQLLNAVSR /(V)	210-226	NAM
1419.785	1419.778	-5.10	(K)/ VCFGIQLLNAVSR /(V)	214-226	
1789.030	1789.044	7.90	(K)/ VC*FGIQLLNAVSR /(V)	214-226	NAM
2076.122	2076.116	-3.00	(K)/ LTVPFLLLQGSADRLCDSK /(G)	234-252	
2445.367	2445.382	6.20	(K)/ LTVPFLLLQGSADRLC*DSK /(G)	234-252	NAM
3534.929	3534.972	12.00	(K)/ LTVPFLLLQGSADRLC*DSKGAYLLMELAK /(S)	234-262	NAM

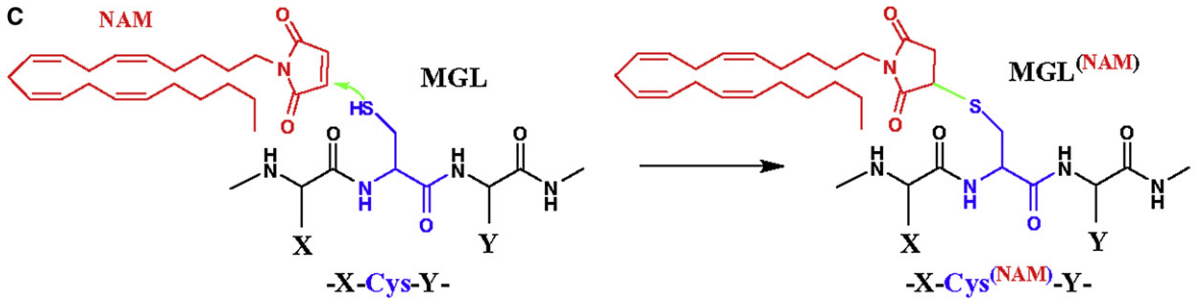

Figure 4. Peptide Fingerprinting of NAM-Inhibited hMGL

(A) The tryptic digest of hMGL inhibited with NAM (at a 33:1 NAM:hMGL molar ratio) was peptide fingerprinted using MALDI-TOF MS. High-resolution MS spectra of NAM-modified peptide ions are shown in the insets.

(B) As identified by MS, the cysteine-containing peptides without or with NAM attached are presented in the table. The cysteines at positions 39, 215, and 249 modified with NAM are shown in bold (C*) and highlighted in green, blue, and red, respectively.

(C) Schematic illustration of MGL alkylation by NAM.

of hMGL inhibition by NAM (Table 1), suggesting that NAM may modify either Cys^{249} or Cys^{215}, but not both in the same hMGL molecule. At the 33:1 NAM:hMGL molar ratio, Cys^{39} also became alkylated, whereas Cys^{208} remained unmodified at all NAM:hMGL molar ratios examined (Table 2). MS/MS analysis of the 1789.04, 2158.28, 2445.37, 3144.55, 3300.75, and 3534.93 *m/z* peptide ions identified Cys^{215}, Cys^{249}, and Cys^{39} as the sites of hMGL alkylation by NAM (data not shown).

(C) Illustration of the carbamylation reaction between the Ser^{129} of hMGL and AM6701.

(D) Schematic presentation of the hMGL catalytic triad within which AM6701 is oriented before (left panel) and after (right panel) hMGL inhibition by Ser^{129} carbamylation (Ser*). The carbons of AM6701 and the MGL peptide bonds are depicted in green and gray, respectively. Blue, nitrogen; white, hydrogen; red, oxygen.

Figure 4C depicts the alkylation reaction between a cysteine residue of hMGL and NAM.

Additional evidence regarding the mechanism of MGL inhibition by NAM was obtained through characterization of cysteine-to-alanine C215A and C249A single and double C215/249A hMGL mutants. Our data indicate that the catalytic activity of the single C215A and C249A mutants and the double C215/249A hMGL mutant did not differ significantly from that of nonmutated hMGL, as indexed by their ability to hydrolyze AHMMCE (data not shown). However, we did observe differences among hMGL and the mutant enzymes in their susceptibility to NAM inhibition (Figure 1C). As evaluated by one-site regression analysis (Figure 1C), elimination of Cys^{249} in either the C249A (IC_{50} = 6.4 μM) or the C215/249A (IC_{50} = 8.5 μM) hMGL mutant reduced the enzyme's sensitivity to NAM as compared with nonmutated hMGL (IC_{50} = 2.8 μM). Due to its biphasic appearance, the NAM concentration-response of the C249A mutant was further analyzed with a two-site equation. The portion of this concentration-response curve (Figure 1C, inset) below the inflection region at ~50% enzyme activity may reflect the partial activity of the C249A mutant alkylated by NAM at Cys^{215}. In marked contrast, the C215A mutant itself was 2-fold more sensitive to NAM (IC_{50} = 1.4 μM) than hMGL (IC_{50} = 2.8 μM). These mutational analyses overall suggest the greater importance of Cys^{249} versus Cys^{215} in hMGL inhibition by NAM.

Our MS and mutation data demonstrate conclusively that hMGL inhibition by NAM depends upon the differential Michael addition of an arachidonylmaleimide group to select cysteine residues in the enzyme. Partial alkylation of hMGL at Cys^{215} and/or Cys^{249} with NAM is sufficient to inhibit hMGL by ~80%, Cys^{249} alkylation being favored, whereas Cys^{39} and Cys^{208} may not be critical. Yet large molar NAM excesses do inhibit hMGL completely (Figure 1C). We hypothesize that, at an 8.3- to 33-fold molar excess of NAM, either Cys^{249} or Cys^{215}, but not both, becomes alkylated in any given hMGL molecule, Cys^{249} preferentially (Table 2). As a consequence of this initial alkylation event, accessibility of the other, unmodified cysteine residue to another NAM molecule is restricted. Because the C215A hMGL mutant was more sensitive to NAM than the nonmutated hMGL, and the C249A mutant was less sensitive to NAM, Cys^{249} alkylation may be the more decisive determinant of hMGL inhibition by NAM (relative to Cys^{215} alkylation). The partial inhibition of MGL in rat cerebellar membranes (Saario et al., 2005) and rat adipocyte fractions (Sakurada and Noma, 1981) by assorted maleimides suggests that our MS and mutational characterization of hMGL-NAM interactions might offer some mechanistic context for MGL inhibition by other *N*-substituted maleimides across species.

SIGNIFICANCE

Detailed mechanistic understanding of the enzymes that deactivate endocannabinoids is a prerequisite for the effective pharmacotherapeutic modulation of the endocannabinoid signaling system. Although extant structural information on MGL relies heavily on provisional modeling studies, the present work has used a ligand-assisted, MS-based approach (termed ligand-assisted protein structure, or "LAPS") augmented with mutational analysis to characterize at the molecular level the mechanisms by which AM6701 and NAM inhibit this critical endocannabinoid-system enzyme responsible for deactivating 2-AG, the most abundant brain endocannabinoid and a full agonist at both cannabinoid receptors. Potent inhibition of hMGL by the carbamyl tetrazole, AM6701, was shown to involve a covalent interaction resulting in selective enzyme carbamylation at Ser^{129} (i.e., Ser^{122} in human MGL) in the GXSXG motif of the MGL catalytic triad. This finding constitutes the first direct confirmation of the essential role of Ser^{129} for MGL hydrolytic activity. Appreciable (~80%) hMGL inhibition by NAM was shown to involve covalent Michael addition of an *N*-arachidonylmaleimide group to Cys^{215} and/or Cys^{249} in hMGL (i.e., Cys^{208} and Cys^{242} in human MGL), somewhat preferentially to the latter cysteine residue. Cys^{39} and Cys^{208} in hMGL (i.e., Cys^{32} and Cys^{201} in human MGL) appear not to play an essential role in partial hMGL inhibition by NAM. Direct demonstration of the involvement of Ser^{129} in hMGL inhibition by AM6701, and Cys^{249} and Cys^{215} in hMGL inhibition by NAM, is useful in designing potent, highly selective MGL-targeted inhibitors as drug candidates to treat disorders (e.g., anxiety, pain, inflammation, and various neurodegenerative diseases) for which potentiating endocannabinoid-system activity might be therapeutic.

EXPERIMENTAL PROCEDURES

Materials

Standard laboratory chemicals, culture media, isopropyl-β-D-thio-galactopyranoside, lysozyme, and DNase I were purchased from Sigma Chemical (St. Louis, MO) and Fisher Chemical (Pittsburgh, PA), unless otherwise specified. SDS-PAGE supplies and Bio Spin™ P-6 columns were from Bio-Rad (Hercules, CA). MS-grade trypsin (Trypsin Gold) was from Promega (Madison, WI). AM6701, AM6702, and AHMMCE were synthesized at the Center for Drug Discovery, Northeastern University, by standard routes that will be detailed elsewhere. Soluble crude rMGL was prepared essentially as described (Goparaju et al., 1998).

Mutant hMGL Preparation and Profiling

The cysteine-to-alanine single C215A and C249A hMGL mutants and the double C215/249A hMGL mutant were generated using the Stratagene QuickChange site-directed mutagenesis kit (La Jolla, CA). The DNA primary structure of all mutants was confirmed by sequencing. The hMGL mutant enzymes were expressed in *E. coli* and assayed for hydrolytic activity with AHMMCE in the absence or presence of NAM at known concentrations, as described below.

Preparative hMGL Purification by Immobilized Metal Affinity Chromatography

A single colony of *E. coli* BL21 (DE3) cells containing the plasmid pET45His6hMGL was inoculated into 12 ml of Luria broth supplemented with ampicillin (100 μg/ml) and grown with shaking at 250 rpm overnight at 37°C. The next morning, 10 ml of this culture was inoculated into 1 L of Luria broth-ampicillin medium, which was incubated with shaking at 37°C until reaching an OD_{600} of 0.6–0.8. Protein expression was induced by adding 1 mM (final concentration) isopropyl-β-D-thio-galactopyranoside. After 5 hr induction, *E. coli* cells were harvested by centrifugation (5,000 g, 10 min, 4°C), washed with PBS buffer, and stored at −80°C. Five grams (wet weight) of cells was resuspended in 50 ml lysis buffer (50 mM Tris [pH 8.0] containing 100 mM NaCl and 0.5% Triton X-100) supplemented with lysozyme (0.2 mg/ml) and DNase I (25 μg/ml) and disrupted on ice by sonication. The sonicate was centrifuged (10,000 g, 30 min, 4°C), and the supernatant was incubated with 1.0 ml (bed volume) pre-equilibrated BD Talon™ metal affinity resin (Takara, Otsu, Shiga, Japan) at room temperature in a rotator. After 1 hr, the suspension was transferred to a gravity-flow column and allowed to settle. The resin was washed with 15 ml lysis buffer, then with 15 ml lysis buffer containing 0.1% Triton X-100 and 10 mM imidazole to elute unbound material. The recombinant

hexa-histidine-tagged human MGL (hMGL) was finally eluted with lysis buffer containing 0.1% Triton X-100 and 200 mM imidazole, and the eluate was collected in 500 μl fractions that were analyzed by SDS-PAGE.

SDS-PAGE and Western Blot Analysis

Samples were denatured at 70°C for 5 min in Laemmli buffer containing 5% β-mercaptoethanol and resolved on 10% PAGE SDS gels. Gels were either stained with Commassie blue or transferred to PVDF membranes for immunodetection with anti-5His horseradish peroxidase conjugate following manufacturer's directions (QIAexpress; QIAGEN, Valencia, CA). Protein bands on the blots were visualized using the ECL Western Blotting Analysis System (GE Healthcare, Piscataway, NJ). A FluorChem Imaging System (Alpha Innotech, San Leandro, CA) was used to photograph developed gels and blots.

Assay of Soluble Crude rMGL and hMGL Hydrolytic Activity

The assay to quantify soluble crude rMGL and hMGL enzymatic activity was based on the hydrolysis of the novel fluorogenic reporter substrate AHMMCE and was performed in a 96-well plate (Costar 3650) format using a Synergy HT Plate Reader (BioTek Instruments, Winooski, VT). To determine overall concentration-response profiles (Figures 1C and 1D), 8 μl *E. coli* lysate containing hMGL (175 ng total protein) with or without designated test compound at specified concentrations in 50 mM Tris-HCl (pH 7.4) containing 8% DMSO was preincubated for 15 min at room temperature. AHMMCE was next added to a final concentration 20 μM in a total volume 200 μl. The incubation was continued for 3 hr, during which fluorescence readings at 360 nm/460 nm ($\lambda_{excitation}/\lambda_{emission}$) were taken every 15 min. Relative fluorescence units were converted to the amount of 7-hydroxy-6-methoxy-4-methylcoumarin (HMC) formed from AHMMCE enzymatic hydrolysis based on a standard fluorescence curve of known amounts of HMC. The HMC formed after 2 hr (i.e., within the linear assay response) was plotted against test-compound concentration, and a nonlinear regression equation was used to determine IC_{50} values (Figure 1D) (Prism software, version 4; GraphPad, San Diego, CA).

Assay of hMGL Inhibition Using AHMMCE

The concentration-dependence of hMGL inhibition (Table 1) was evaluated after incubation of purified hMGL with test compound for 1 hr at room temperature. The assay was performed in a 96-well format (Costar 3795) in 10 mM Tris-HCl (pH 8.0) containing 5% DMSO (final volume 20 μl) with hMGL alone (1 ng) and hMGL (3 ng) that had been incubated with test compound at a known molar ratio to hMGL enzyme, as specified in Table 1. AHMMCE (50 or 100 μM) was then added as fluorogenic reporter substrate. The plate was exposed to ultraviolet light (360 nm) for 3 s, and images were recorded at the start of the assay and every 10 min thereafter for 1 hr using a FluorChem Imaging System. The brightness of each well was quantified with FluorChem Imaging System Software and normalized to enzyme concentration, and the percent enzyme inhibition was determined. The intensity of light emission was proportional to the amount of functional enzyme and correlated negatively with the test compound's effectiveness as hMGL inhibitor.

Interaction of Inhibitors with hMGL and Preparation of Peptide Hydrolysates for MALDI-TOF MS

Purified hMGL (3.1 μg, 3 μM) in 10 mM Tris-HCl ([pH 8.0], (30 μl) was incubated for 1 hr at room temperature without or with test compound present at a known molar ratio to hMGL. After evaluation of hMGL inhibition by AM6701 or NAM (above), the incubation was terminated by rapid desalting with a Bio-Spin 6 column in 50 mM ammonium bicarbonate buffer containing 0.02% CYMAL (pH 8.0). The desalted hMGL was digested with trypsin (200 ng) overnight either directly or after reduction alkylation under mild conditions at room temperature with dithiothreitol (17 mM for 30 min) and iodoacetamide (55 mM for 1 hr in the dark; Zvonok et al., 2007).

MALDI-TOF MS Analysis

All MS data were acquired on a 4800 Maldi TOF/TOF mass spectrometer (Applied Biosystems, Framingham, MA) fitted with a 200 Hz solid-state ultraviolet laser (wavelength 355 nm) from samples spotted on Opti-TOF® 384-well plate inserts. Each sample of protein digest was crystallized by spotting 0.5 μl tryptic digest and 0.5 μl α-cyano-4-hydroxycinnamic acid matrix (5 mg/mL in aqueous 60% acetonitrile/0.1% trifluoroacetic acid). After crystallization, the dried spot was washed with 5 μl aqueous 0.1% trifluoroacetic acid for rapid desalting. In those cases where trace residual salt and detergent suppressed signal, the digest was diluted 10-fold with matrix solution, and 1 μl of the diluted digest was spotted for analysis. Spectra were acquired by accumulating data from several positions within each sample well to determine the ions present. All MS spectra were externally calibrated using a mixture of peptide standards (des-Arg1-bradykinin at MH^+ 904.4681; angiotensin I at MH^+ 1296.6853; Glu-fibrino peptide at MH^+ 1570.6774; ACTH [clip 1–17] at MH^+ 2093.0867; ACTH [clip 18–39] at MH^+ 2465.1989; and ACTH [clip 7–38] at MH^+ 3657.9294). MS/MS spectra were acquired on selected ions of interest. The instrument was calibrated in the MS/MS mode using five daughter ions (at *m/z* 175.119, 684.346, 813.389, 1056.475, and 1441.634) generated from the fragmentation of Glu-fibrino peptide (MH^+ 1570.6774.) MS/MS spectra were acquired under the following conditions: precursor isolation resolution of 200; collision energy of 2 kV; cell pressure of 2×10^{-5} torr; air as collision gas. Accumulation was performed until spectra were of optimal quality.

Data analyses were performed by comparing the monoisotopic peaks with the theoretical molecular weights corresponding to the expected peptide digestion products. The maximum error allowed was set to 100 ppm. Theoretical molecular weights of expected peptides after digestion were calculated using MS-Digest (University of California, San Francisco, Mass Spectrometry Facility, San Francisco, CA) and FindPept and FindMod tools (ExPASy server, Swiss Institute of Bioinformatics, Geneva, Switzerland).

ACKNOWLEDGMENTS

We thank Jing Li for experimental assistance. This work was supported by the National Institute on Drug Abuse, National Institutes of Health grants DA09158, DA00493, DA03801, DA07215, and DA07312 to A.M.

Received: February 7, 2008
Revised: June 9, 2008
Accepted: June 23, 2008
Published: August 22, 2008

REFERENCES

Alexander, J.P., and Cravatt, B.F. (2006). The putative endocannabinoid transport blocker LY2183240 is a potent inhibitor of FAAH and several other brain serine hydrolases. J. Am. Chem. Soc. *128*, 9699–9704.

Blankman, J.L., Simon, G.M., and Cravatt, B.F. (2007). A comprehensive profile of brain enzymes that hydrolyze the endocannabinoid 2-arachidonoylglycerol. Chem. Biol. *14*, 1347–1356.

Cravatt, B.F., Giang, D.K., Mayfield, S.P., Boger, D.L., Lerner, R.A., and Gilula, N.B. (1996). Molecular characterization of an enzyme that degrades neuromodulatory fatty-acid amides. Nature *384*, 83–87.

Di Marzo, V., and Petrosino, S. (2007). Endocannabinoids and the regulation of their levels in health and disease. Curr. Opin. Lipidol. *18*, 129–140.

Deutsch, D.G., Lin, S., Hill, W.A., Morse, K.L., Salehani, D., Arreaza, G., Omeir, R.L., and Makriyannis, A. (1997). Fatty acid sulfonyl fluorides inhibit anandamide metabolism and bind to the cannabinoid receptor. Biochem. Biophys. Res. Commun. *231*, 217–221.

Devane, W.A., Hanus, L., Breuer, A., Pertwee, R.G., Stevenson, L.A., Griffin, G., Gibson, D., Mandelbaum, A., Etinger, A., and Mechoulam, R. (1992). Isolation and structure of a brain constituent that binds to the cannabinoid receptor. Science *258*, 1946–1949.

Dinh, T.P., Kathuria, S., and Piomelli, D. (2004). RNA interference suggests a primary role for monoacylglycerol lipase in the degradation of the endocannabinoid 2-arachidonoylglycerol. Mol. Pharmacol. *66*, 1260–1264.

Ghafouri, N., Tiger, G., Razdan, R.K., Mahadevan, A., Pertwee, R.G., Martin, B.R., and Fowler, C.J. (2004). Inhibition of monoacylglycerol lipase and fatty acid amide hydrolase by analogues of 2-arachidonoylglycerol. Br. J. Pharmacol. *143*, 774–784.

Goparaju, S.K., Ueda, N., Yamaguchi, H., and Yamamoto, S. (1998). Anandamide amidohydrolase reacting with 2-arachidonoylglycerol, another cannabinoid receptor ligand. FEBS Lett. *422*, 69–73.

Karlsson, M., Contreras, J.A., Hellman, U., Tornqvist, H., and Holm, C. (1997). cDNA Cloning, tissue distribution, and identification of the catalytic triad of monoglyceride lipase. J. Biol. Chem. *272*, 27218–27223.

Malan, T.P., Jr., Ibrahim, M.M., Lai, J., Vanderah, T.W., Makriyannis, A., and Porreca, F. (2003). CB2 cannabinoid receptor agonists: pain relief without psychoactive effects? Curr. Opin. Pharmacol. *3*, 62–67.

Mechoulam, R., Ben-Shabat, S., Hanus, L., Ligumsky, M., Kaminski, N.E., Schatz, A.R., Gopher, A., Almog, S., Martin, B.R., Compton, D.R., et al. (1995). Identification of an endogenous 2-monoglyceride, present in canine gut, that binds to cannabinoid receptors. Biochem. Pharmacol. *50*, 83–90.

Moore, S.A., Nomikos, G.G., Dickason-Chesterfield, A.K., Schober, D.A., Schaus, J.M., Ying, B.-P., Xu, Y.-C., Phebus, L., Simmons, R.M.A., Li, D., et al. (2005). Identification of a high-affinity binding site involved in the transport of endocannabinoids. Proc. Natl. Acad. Sci. USA *102*, 17852–17857.

Muccioli, G.G., Xu, C., Odah, E., Cudaback, E., Cisneros, J.A., Lambert, D.M., López Rodríguez, M.L., Bajjalieh, S., and Stella, N. (2007). Identification of a novel endocannabinoid-hydrolyzing enzyme expressed by microglial cells. J. Neurosci. *27*, 2883–2889.

Ortar, G., Cascio, M.G., Moriello, A.S., Camalli, M., Morera, E., Nalli, M., and Di Marzo, V. (2008). Carbamoyl tetrazoles as inhibitors of endocannabinoid inactivation: A critical revisitation. Eur. J. Med. Chem. *43*, 62–72.

Pacher, P., Batkai, S., and Kunos, G. (2006). The endocannabinoid system as an emerging target of pharmacotherapy. Pharmacol. Rev. *58*, 389–462.

Saario, S.M., and Laitinen, J.T. (2007). Therapeutic potential of endocannabinoid-hydrolysing enzyme inhibitors. Basic Clin. Pharmacol. Toxicol. *101*, 287–293.

Saario, S.M., Salo, O.M., Nevalainen, T., Poso, A., Laitinen, J.T., Jarvinen, T., and Niemi, R. (2005). Characterization of the sulfhydryl-sensitive site in the enzyme responsible for hydrolysis of 2-arachidonoylglycerol in rat cerebellar membranes. Chem. Biol. *12*, 649–656.

Saario, S.M., Poso, A., Juvonen, R.O., and Salo-Ahen, O.M.H. (2006). Fatty acid amide hydrolase inhibitors from virtual screening of the endocannabinoid system. J. Med. Chem. *49*, 4650–4656.

Sakurada, T., and Noma, A. (1981). Subcellular localization and some properties of monoacylglycerol lipase in rat adipocytes. J. Biochem. *90*, 1413–1419.

Smyth, D.G., Nagamatsu, A., and Fruton, J.S. (1960). Some reactions of N-ethylmaleimide. J. Am. Chem. Soc. *82*, 4600–4604.

Sugiura, T., Kondo, S., Sukagawa, A., Nakane, S., Shinoda, A., Itoh, K., Yamashita, A., and Waku, K. (1995). 2-Arachidonoylglycerol: a possible endogenous cannabinoid receptor ligand in brain. Biochem. Biophys. Res. Commun. *215*, 89–97.

Vemuri, V.K., Janero, D.R., and Makriyannis, A. (2008). Pharmacotherapeutic targeting of the endocannabinoid signaling system: Drugs for obesity and the metabolic syndrome. Physiol. Behav. *93*, 671–686.

Wei, B.Q., Mikkelsen, T.S., McKinney, M.K., Lander, E.S., and Cravatt, B.F. (2006). A second fatty acid amide hydrolase with variable distribution among placental mammals. J. Biol. Chem. *281*, 36569–36578.

Zvonok, N., Yaddanapudi, S., Williams, J., Dai, S., Dong, K., Rejtar, T., Karger, B.L., and Makriyannis, A. (2007). Comprehensive proteomic mass spectrometric characterization of human cannabinoid CB2 receptor. J. Proteome Res. *6*, 2068–2079.

Zvonok, N., Williams, J., Johnston, M., Pandarinathan, L., Janero, D.R., Li, J., Krishnan, S.C., and Makriyannis, A. (2008). Full mass spectrometric characterization of human monoacylglycerol lipase generated by large-scale expression and single-step purification. J. Proteome Res. *7*, 2158–2164.

